JOURNAL OF Materials CHEMISTRY

Cation distribution and magnetic structure of the ferrimagnetic spinel $NiCo_2O_4$

José F. Marco,*[a] J. Ramón Gancedo,[a] Mercedes Gracia,[a] Juan Luis Gautier,[b] Edmundo I. Ríos,[b] Helen M. Palmer,[c] Colin Greaves[c] and Frank J. Berry[d]

[a]*Instituto de Química-Física "Rocasolano", CSIC, c/ Serrano 119, 28006 Madrid, Spain. E-mail: jfmarco@iqfr.csic.es*
[b]*Facultad de Química y Biología, Universidad de Santiago de Chile, Av. L. O'Higgins, 3363 Santiago, Chile*
[c]*School of Chemistry, University of Birmingham, Edgbaston, Birmingham, UK B15 2TT*
[d]*Department of Chemistry, The Open University, Walton Hall, Milton Keynes, UK MK7 6AA*

Received 6th April 2001, Accepted 17th August 2001
First published as an Advance Article on the web 9th October 2001

The compound $NiCo_2O_4$, with spinel-related structure, has been prepared by thermal decomposition of metal nitrates and its bulk structural properties examined by means of magnetic measurements, neutron diffraction, X-ray absorption near edge structure (XANES) and extended X-ray absorption fine structure (EXAFS). The results suggest a delocalised electron distribution on the octahedral sites with average oxidation states of $+3.5$ and $+2.5$ for nickel and cobalt, respectively, and lead to a cation distribution for $NiCo_2O_4$ of $\{Ni^{3+}_{0.1}Co^{2+}_{0.9}\}_{tet}[Ni^{3.5+}_{0.9}Co^{2.5+}_{1.1}]_{oct}O_4$. This electronic configuration is consistent with magnetisation measurements if applied magnetic fields cause a charge redistribution on the octahedral sites to favour Co^{3+} and Ni^{3+}. The surface of $NiCo_2O_4$ was examined by X-ray photoelectron spectroscopy (XPS) and found to have a different composition containing Co^{2+}, Co^{3+}, Ni^{2+}, Ni^{3+} and, probably, Ni^{4+}.

Introduction

The activity of nickel cobaltite, $NiCo_2O_4$, as a bifunctional catalyst for oxygen reduction,[1–3] and for reduction in alkaline media[4,5] and as an electrode for organic electrosynthesis[6] is well established.

$NiCo_2O_4$ is generally regarded[7] as adopting a spinel-related structure in which nickel occupies the octahedral sites and cobalt is distributed over both octahedral and tetrahedral sites. However, the detailed description of the distribution of the cationic sites is a matter of some uncertainty.[8,9] This, to some extent, reflects the instability of $NiCo_2O_4$ in air at temperatures exceeding 400 °C, which results in the material requiring synthesis at low temperatures. $NiCo_2O_4$ is known to have unusual magnetic properties with magnetisation in fields of $\sim$0.8 T, extrapolated to 0 K, corresponding to moments of $\sim$1.25–1.5 μ_B per formula unit.[7,10,11] However, no simple cation and electronic distribution in the spinel structure can rationalise such moments: for example, the chemically plausible description of tetrahedral high spin Co^{2+} ($e_g^4t_{2g}^3$) with octahedral low spin Co^{3+} (t_{2g}^6) and Ni^{3+} ($t_{2g}^6e_g^1$) should give a spontaneous magnetisation at 0 K of 2 μ_B per formula unit. In addition, the experimental magnetisation has been found not to saturate at fields of $\sim$1.1 T.[7,10] These problems prompted a neutron powder diffraction study by Battle *et al.*,[9] which provides a reasonable, but probably incomplete, explanation of the magnetic data. Some degree of cation intermixing was found (92% Co and 8% Ni on the tetrahedral sites) and field dependence of the magnetisation data was attributed to a field-dependent electronic distribution. Essentially, the model requires low spin electronic configurations for all ions on both tetrahedral and octahedral sites: the octahedral Co^{3+} ions are diamagnetic so that the magnetisation was attributed to tetrahedral $Co^{(2+\delta)+}$,containing $3-\delta$ unpaired electrons, and octahedral $Ni^{(3-\delta)+}$, with $1+\delta$ unpaired electrons. This description predicts a spontaneous moment of between 0 μ_B ($\delta=1$) and 2 μ_B ($\delta=0$), and the magnetisation data therefore requires the amount of charge transfer, δ, to decrease with the applied field. Although consistent with experimental measurements, this interpretation was founded on the assumption that the electron pairing energy for all ions is less than the crystal field splitting. This is certainly justified for the octahedral cations but is doubtful for the tetrahedral site, even for Co^{3+} species.

In view of the prevailing uncertainty concerning the magnetic and electronic nature of $NiCo_2O_4$, and our recent finding[12] that the bulk cationic distribution depends on the synthesis procedure, we have conducted a detailed study of the structure and properties of $NiCo_2O_4$. Here we report the characteristics of $NiCo_2O_4$ prepared by thermal decomposition of nitrates, as determined by magnetic measurements, neutron powder diffraction, X-ray absorption near edge structure (XANES), extended X-ray absorption fine structure (EXAFS) and X-ray photoelectron spectroscopy (XPS).

Experimental

$NiCo_2O_4$ was synthesised by thermal decomposition of metal nitrates. An acidified solution (1 ml of concentrated HNO_3/100 ml of distilled water) of cobalt- and nickel-nitrates (2 : 1 molar ratio) was dried in a sand bath at 140 °C. The ground residue was heated under a stream of oxygen at 200 °C with frequent shaking for 24 h, and for another 46 h at 320 °C. The product was allowed to cool slowly. X-Ray powder diffraction data showed the material be single phase. Elemental analyses by atomic absorption spectroscopy (AAS) performed on six different samples of the oxide gave a Co/Ni ratio ranging from 1.97 to 2.00, *i.e.* 1% within the nominal composition. SEM examination showed the material to consist of uniform, small round particles that sometimes agglomerate to form larger particles (Fig. 1). Energy dispersive X-ray analysis showed the sample to be homogeneous from particle to particle with an

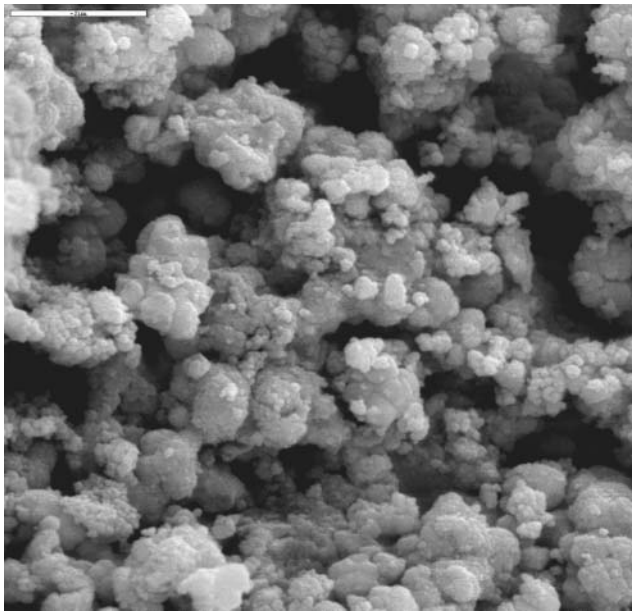

Fig. 1 SEM micrograph recorded from $NiCo_2O_4$. The length of the white line in the upper left corner corresponds to 2 μm.

average Co/Ni ratio of 1.87, *i.e.* 7% within the nominal composition. The discrepancy between the analytical data recorded by EDX and AAS analyses might reflect the lower accuracy of EDX in this case when examining the small particles (<1 μm) of $NiCo_2O_4$ (Fig. 1).

Magnetisation data were collected as a function of field and temperature using an Oxford Instruments 12 Tesla VSM. Data were collected at regular intervals in the range 4–275 K whilst the field was swept between 0–12 T at each temperature. Neutron powder diffraction data were collected at 4 K on the diffractometer POLARIS at ISIS, Rutherford Appleton Laboratory, UK. Both backscattering, (high resolution, C-bank), and low angle (low resolution, A-bank) data sets were used simultaneously in the structure refinements (GSAS software)[13] to maximise information on crystallographic (C-bank) and magnetic structures (A-bank which provides information at lower Q).

XANES and EXAFS measurements were performed on station 7.1 at the Synchrotron Radiation Source at Daresbury Laboratory operating at an energy of 2.0 GeV and an average current of 200 mA. Data were collected at 298 K using a Si(111) double crystal order sorting monochromator in transmission mode using 20% harmonic rejection. The energy scale was calibrated using a 6 μm nickel foil in the case of the nickel K-edge and a 6 μm cobalt foil for the cobalt K-edge. The position of the nickel foil edge was taken at 8332.8 eV and that of the cobalt foil edge was at 7708.9 eV. All the nickel and cobalt XANES data were referred to these two values. All the edges were recorded at least twice and at different times separated by several hours but within the lifetime of the beam. The reproducibility in the determination of the edge positions was found to be better than 0.2 eV. The edge profiles were separated from the EXAFS data and, after subtraction of the linear pre-edge background, normalized to the edge step. The positions of the edge maxima were obtained from the zeros of the first derivative of the edge profile and the position of the edges themselves was taken at the energy at which the normalized absorption was 0.5 (*i.e.* the absorption at half-height of the edge step). The EXAFS oscillations were isolated after background subtraction of the raw data using the Daresbury program EXBACK and converted into k space. The data were weighted by k^3, where $\boldsymbol{k}$ is the photoelectron wavevector, to compensate for the diminishing amplitude of the EXAFS at high k. The data were fitted using the non-linear squares minimisation program EXCURV90[14] which calculates the theoretical function using the fast curved wave theory.[15] The phase shifts were calculated from *ab initio* methods as described elsewhere[16] and tested on NiO and CoO, the results being in reasonable agreement with the published crystallographic data (differences in first-shell distances were less than 0.02 Å).[17,18] The quality of the fit to the data was assessed by using statistical tests[19] and found to be significant at the 1% level.

XPS data were recorded with a triple channeltron CLAM2 analyzer under a vacuum better than 1×10^{-8} Torr using Al-Kα radiation and a constant analyzer transmission energy of 20 eV. All the spectra were recorded at a take-off angle of 90°. All binding energy values were charge-corrected to the C 1s signal (284.6 eV). All the spectra were computer fitted and the binding energies are accurate to ±0.2 eV. Relative atomic concentrations were calculated using tabulated atomic sensitivity factors.[20]

Results and discussion

(i) Magnetisation measurements

Fig. 2(a) shows magnetisation *versus* field at various temperatures in the range 4–280 K. In accordance with previous reports,[7,10] it is seen that complete saturation is not achievable

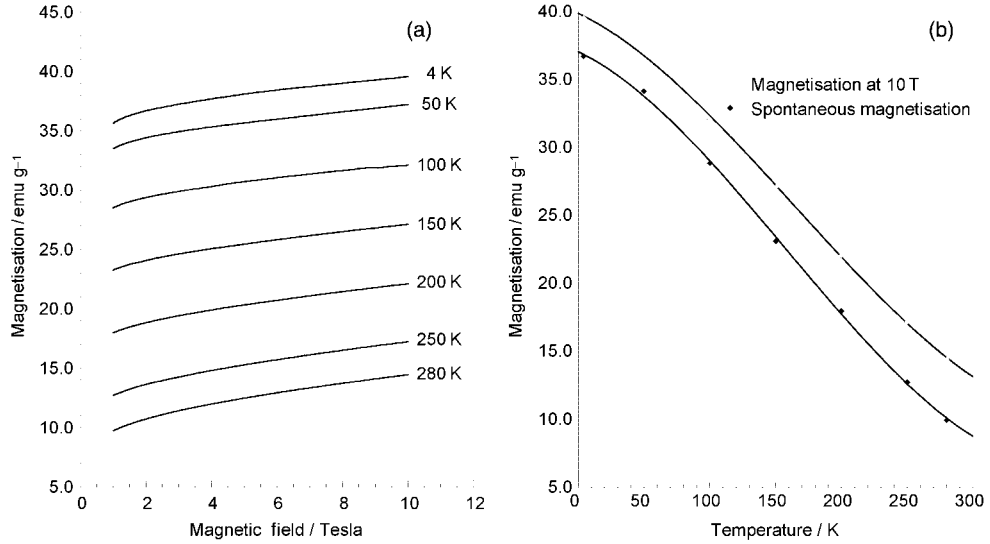

Fig. 2 Plots of (a) magnetisation against field and (b) magnetisation (at 10 T and spontaneous) against temperature.

even in fields as high as 10 T. The magnetisation at 10 T is plotted against temperature in Fig. 2(b) and at this field, the magnetisation at 4 K corresponds to a moment of 1.71 μ_B per formula unit. This is significantly higher than the moments previously reported (1.25 μ_B[7] and 1.5 μ_B[10,11]), but these were determined in much lower fields, $\sim$0.8 T. A more meaningful comparison is given by the magnetisation at 0.8 T in Fig. 2(a), which gives a moment of 1.52 μ_B, somewhat higher than that obtained by Knop *et al.*[7] but in good agreement with that calculated by Blasse[11] from the earlier data of Lotgering.[10] In addition to the moment at 10 T, Fig. 2(b) also shows the variation of spontaneous moment with temperature; these data were obtained by extrapolating the linear part of the magnetisation curves to $H=0$ T. The spontaneous moment at 4 K was 1.58 μ_B and the remanent moment at 4 K, obtained from extrapolation of low field data (not shown in Fig. 2(a)) to $H=0$ T, is 0.64 μ_B. The temperature variation of magnetisation shown in Fig. 2(b) displays a similar anomalous shape to that previously reported,[7] and is consistent with a field dependent electronic configuration, previously suggested by Battle *et al.*[9] In order to probe the local moments on the cation sites in $NiCo_2O_4$, neutron powder diffraction data were collected at 4 K.

(ii) Neutron powder diffraction

Refinement of the crystallographic structure was initially based solely on the C-bank data, which provides high-Q information and is therefore insensitive to magnetic scattering effects. It was immediately apparent that although the tetrahedral sites were predominantly occupied by Co, a small amount of mixing was present to give *ca.* 10% Ni at these sites. This level of intermixing is the same as previously reported.[9]

The magnetic structure was investigated using both C- and A-banks. Given the uncertainty surrounding the cation oxidation states on the two cation sites, we were unable to provide an unequivocal form factor for each position. However, in the final stages of the refinement, we demonstrated that the refined magnetic moments on the two sites were insensitive to the form factors examined (Co^{2+}, Ni^{2+}, Co^{3+}, Ni^{3+}) within the statistical esd of the moments. The data reported below were all obtained using the Co^{2+} form factor[21] for both tetrahedral and octahedral sites.

The refinement clearly confirmed the expected ferrimagnetic order on the tetrahedral and octahedral sites, with moments of +2.18(9) μ_B and −1.49(8) μ_B respectively. The refined data are given in Table 1 and the neutron diffraction profiles are shown in Fig. 3. Small additional peaks ($d\sim2.0$ Å) in the neutron profiles are primarily from the cryostat; they were considered not large enough to warrant exclusion from the refinement. For the tetrahedral cations, the average metal–oxygen distance is calculated to be 1.9182(4) Å and the equivalent distance for the octahedral cations is slightly larger, 1.9397(2) Å.

The tetrahedral moment is, within statistical error, identical to that obtained by Battle *et al.*[9] (2.29(9) μ_B), whereas the previously reported[9] octahedral moment (−0.97(13) μ_B) is smaller than that found in the present study, although the difference amounts to little more than three esds. In contrast with the earlier data,[9] which suggested a spontaneous moment of 0.35(28) μ_B with the tetrahedral moments dominant, the current refinement gives an overall moment of 0.80(18) μ_B, with the octahedral moments dominant. It is clear that the net moment is significantly lower than the spontaneous moment, and is similar to the remanent moment indicated by the magnetisation measurements. It is therefore likely that a major contributing factor to the field dependence of the magnetisation is a field-dependent electronic redistribution as previously suggested.[9] It is impossible to provide a convincing electronic model based solely on the results of the neutron diffraction refinement, although the tetrahedral moment strongly suggests that species with three unpaired electrons (high spin Co^{2+}, high spin Ni^{3+}) are dominant in these sites. In order to provide information on the cation oxidation states, XANES and EXAFS data were collected.

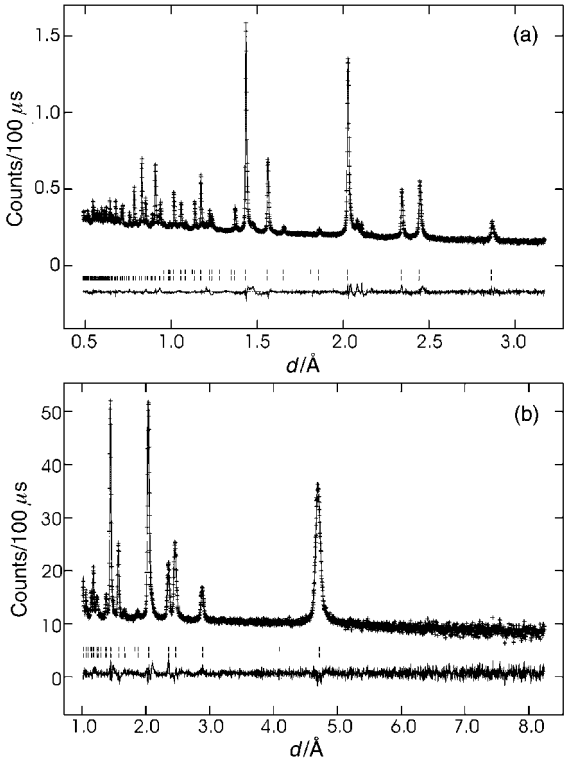

Fig. 3 Fitted neutron diffraction profiles showing observed (dots), calculated and difference (solid lines) data: (a) C-bank, (b) A-bank.

(iii) XANES and EXAFS

The nickel K-edge XANES recorded from nickel cobaltite, $NiCo_2O_4$, metallic nickel and nickel oxide, NiO, are shown in Fig. 4. The absence in the XANES recorded from $NiCo_2O_4$ of well-defined pre-edge features suggests that nickel, as expected, is predominantly located in the octahedral sites. The shift of the nickel absorption edge of $NiCo_2O_4$ with respect to the edge of metallic nickel is *ca.* 5.3 eV (Table 2). It is known that an increase in a unit of the oxidation state of nickel in nickel-containing compounds corresponds to a shift of *ca.* 1.5 eV in the position of the absorption edge.[22–26] In fact the edge shifts of Ni^{3+}-containing compounds such as β-NiOOH, $LaNiO_3$ and $LiNiO_2$ with respect to the edge of metallic nickel are 4.5 eV,[22] 4.5 eV[27] and 3.9 eV,[25] respectively, whilst the corresponding edge shifts of Ni^{4+}-containing compounds such as

Table 1 Refined structural parameters for $NiCo_2O_4$ at 4 K. Space group *Fd3m*, $a=8.1138(2)$ Å; $R_{wp}=1.97\%$ (C-bank), 3.48% (A-bank); $\chi^2=6.44$

Atom	*x*	*y*	*z*	$100U_{iso}$/Å^2	Occupancy	μ/μ_B
Co/Ni(1)[a]	0.125	0.125	0.125	0.63(3)	0.90(2)/0.10(2)	2.18(9)
Co/Ni(2)[a]	0.5	0.5	0.5	0.48(2)	0.552(1)/0.448(1)	−1.49(8)
O	0.26149(3)	0.26149(3)	0.26149(3)	0.49(1)		

[a]Co/Ni(1) are tetrahedral, Co/Ni(2) are octahedral.

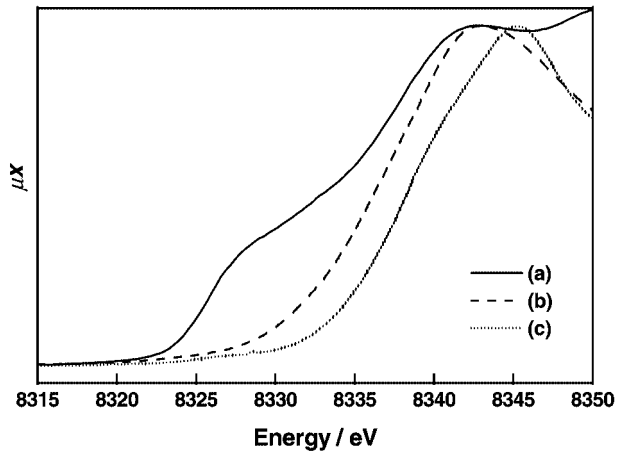

Fig. 4 Ni K-edge XANES data: (a) Ni metal, (b) NiO, (c) $NiCo_2O_4$.

Table 2 Ni K-edge positions

Sample	Edge position/eV	Δ^a/eV	Edge maximum/eV
Ni	8332.8	—	—
NiO	8336.1	3.4	8343.0
$NiCo_2O_4$	8338.1	5.3	8345.3

[a] Δ is the energy difference between the position of the edge in the compound and that of Ni metal. The position of the edges was taken at the energy at which the normalized absorption was 0.5 (*i.e.* the absorption at half-height of the edge step).

$BaNiO_3$ and $KNiIO_3$ are 6.0[22] and 6.2 eV,[25] respectively. Taking this into account the XANES results suggest that nickel in $NiCo_2O_4$ prepared by thermal decomposition of metal nitrates is present in an average oxidation state of about +3.5[22] or, in other words, it would contain both Ni^{3+} and Ni^{4+}.

The Ni K-edge EXAFS recorded from $NiCo_2O_4$ was initially fitted to a simple model consisting of a first coordination shell of six oxygen atoms. Given the inherent difficulties in accurately determining coordination numbers in EXAFS, the small amount of nickel that neutron diffraction has shown to be present in tetrahedral sites was not taken into account when fitting the EXAFS. The fit gave a Ni–O distance of 1.93 Å which is within the range of the Ni–O distances previously observed[24,28–32] in mixed valent Ni^{3+}–Ni^{4+} systems. This distance is also in fairly good agreement with that obtained from the neutron diffraction data for the octahedral cations. Given that the XANES results point out to the presence of some Ni^{4+} in $NiCo_2O_4$ prepared by thermal decomposition of metal nitrates, a second fitting model was adopted. In this second model the first coordination shell was split in two shells of oxygen atoms at distances of 1.88 Å (characteristic of Ni^{4+} in octahedral oxygen coordination[22]) and 1.96 Å (a distance which seems to be reasonable for Ni^{3+} in octahedral oxygen coordination[24,25,30,33–35]). In the first steps of fitting these distances were kept fixed and the coordination numbers and Debye–Waller factors were allowed to refine. Finally the coordination numbers obtained were approximated to the nearest half-integers and the distances and Debye–Waller factors were allowed to refine. This fit was slightly better than the fit considering only a single Ni–O distance. The results are summarised in Fig. 5 and Table 3. The ratio of occupation numbers corresponding to each distance can be used to estimate the ratio of the different nickel oxidation states. In our case this ratio (1.5 : 5.5) is indicative of nickel being in an average oxidation state of +3.2. We would comment however that, given the large number of parameters involved in the fit of the EXAFS, the fit may be not unique and other combinations of Ni–O distances and coordination numbers different to the ones presented here can also give a reasonable fitting index. In our view, the important points raised from the Ni K-edge XANES and EXAFS recorded from the $NiCo_2O_4$ prepared by thermal decomposition of metal nitrates are:

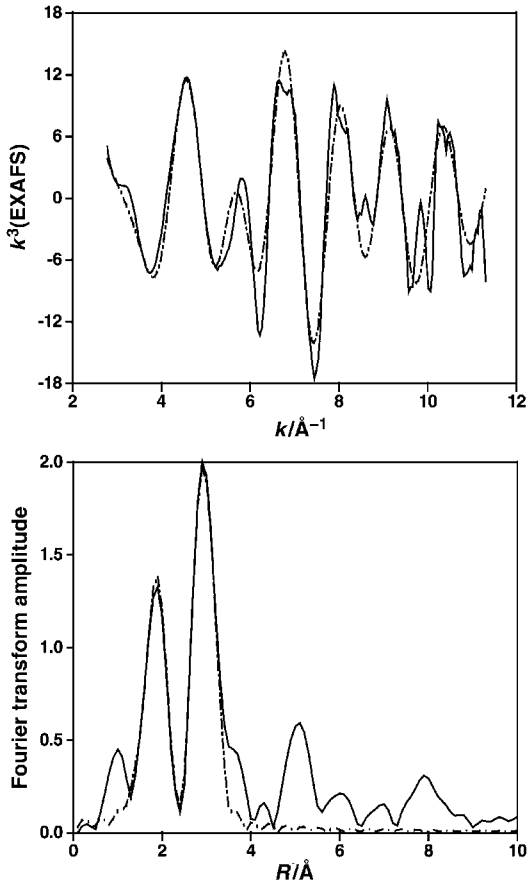

Fig. 5 Ni K-edge EXAFS data (top) and corresponding Fourier transform (bottom). The broken line shows the result of the fit.

Table 3 Final fitting parameters obtained from the fit of the Ni K-edge EXAFS considering two first Ni–O shells

Atom type	Coordination number	Distance/Å	$2\sigma^2$/Å^2
O	1.5	1.88	0.008
O	5.5	1.96	0.023
Ni	6	2.81	0.034
Co	6	2.89	0.013

(1) the shift of the absorption edge with respect to the edge of metallic nickel that is considerably higher than that usually shown by Ni^{3+}-containing compounds.

(2) a shorter average Ni–O distance of 1.93 Å in the first coordination shell than that expected (1.95–1.97 Å) for a low-spin Ni^{3+} ion in octahedral oxygen coordination.

Taken together, both factors point to the existence of some Ni^{4+} ions in this compound.

This surprising and significant result raises serious doubts about all previous attempts to rationalise the unusual magnetic behaviour of $NiCo_2O_4$, since none has been consistent with such a high nickel oxidation state. Moreover, given the chemical composition, the presence of such a state demands the presence of some Co^{2+} and the co-existence of both Co^{2+} and Ni^{4+} (or a mixed valent $Ni^{3.5+}$) requires careful consideration and justification. The possibility of such highly oxidised Ni on the octahedral sites allowed further analysis of the magnetic moments determined by neutron diffraction.

The tetrahedral moment of 2.18 μ_B is consistent with a d^7 electron configuration allowing for covalence and zero-point

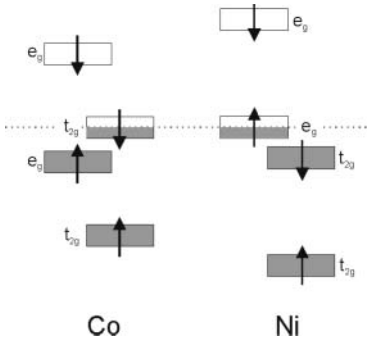

Fig. 6 Schematic representation of the proposed band description of the octahedral cations showing overlap of the Co minority spin t_{2g} band with the Ni majority spin e_g band.

spin deviations. The dominant Co ion in this site is therefore Co^{2+}, and given the high Ni oxidation state implied by XANES, it is highly likely that the Ni on this site is Ni^{3+}, also having a d^7 configuration, which will be high spin in a tetrahedral oxide environment. The octahedral moment of $-1.49\ \mu_B$ suggests approximately two unpaired electrons per site. The presence of mainly Co^{3+} (d^6) and Ni^{3+} (d^7), which are both expected to be low spin in this environment would, however, give a moment corresponding to only 0.5 electrons per site. Given the XANES data, we therefore suggest some band overlap involving the octahedral cations, which results in electron transfer from Ni to Co to provide $Ni^{(3+\delta)+}$ and $Co^{(3-\delta)+}$. Since Co^{3+} in oxide environments is often near the border between high and low spin, we propose that the charge transfer causes the octahedral Co species now to be high spin; $Ni^{(3+\delta)+}$ will clearly remain low spin. If the degree of band overlap, and hence charge distribution, is field dependent, we would expect field-dependent magnetisation caused effectively by a change in the electron configurations with extremes represented by $\delta=0$, Co^{3+} $(t_{2g}^4e_g^2)/Ni^{3+}(t_{2g}^6e_g^1)$, and $\delta=1$, $Co^{2+}(t_{2g}^5e_g^2)/Ni^{4+}(t_{2g}^6e_g^0)$. This description suggests a band description involving overlap of the minority spin t_{2g} Co levels with the majority spin e_g Ni levels, as indicated in Fig. 6. The net moment per formula unit, ignoring the small effects associated with cation mixing, is then 2.0 μ_B for $\delta=0$ and 0 μ_B for $\delta=1$. For $\delta=0.5$, the octahedral moment would correspond to two unpaired electrons per site, giving a net moment of 1.0 μ_B per formula. This configuration, corresponding to an ideal composition $\{Co^{2+}\}_{tet}[Co^{2.5+}Ni^{3.5+}]_{oct}$, is therefore consistent with both the neutron diffraction and XANES data; the magnetisation data suggests quite a large decrease in δ at quite small applied fields. This large effect is unusual and would be expected only for very narrow band Mott insulators.

The cobalt K-edge XANES (Fig. 7) showed a clear pre-edge feature at 7706.3 eV indicating that cobalt occupies the tetrahedral sites of the spinel-related $NiCo_2O_4$ structure. This is also consistent with the neutron diffraction data. The shift of the cobalt K-edge position with respect to that of cobalt metal is higher than that recorded from CoO (Fig. 7, Table 4) suggesting that the average oxidation state of cobalt in $NiCo_2O_4$ prepared by thermal decomposition of metal nitrates is higher than +2.

The cobalt–oxygen distances of 1.88 and 1.92 Å (Table 5) derived from the cobalt K-edge EXAFS (Fig. 8) agree with those determined by neutron diffraction from cobalt in tetrahedral- and octahedral-coordination, respectively. The ratio of tetrahedral- to octahedrally-coordinated cobalt of *ca.*

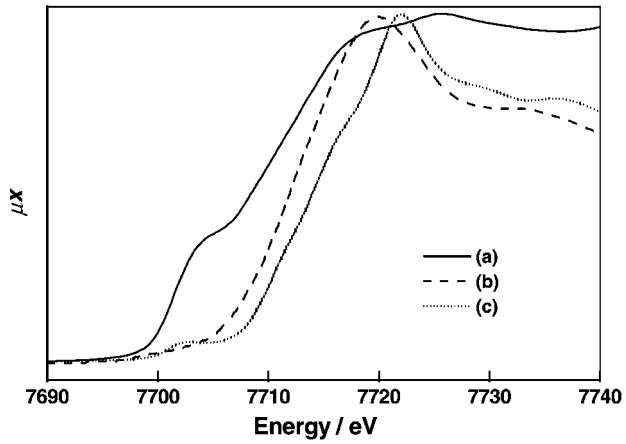

Fig. 7 Co K-edge XANES data: (a) Co metal, (b) CoO, (c) $NiCo_2O_4$.

Table 4 Co K-edge positions

Sample	Edge position/eV	Δ^a/eV	Edge maximum/eV
Co	7708.9	—	—
CoO	7712.2	3.3	7720.1
$NiCo_2O_4$	7714.0	5.1	7722.5

[a] Δ is the energy difference between the position of the edge in the compound and that of Co metal.

Table 5 Final fitting parameters obtained from the fit of the Co K-edge EXAFS

Atom type	Coordination number	Distance/Å	$2\sigma^2$/Å^2
O	2.3	1.88	0.003
O	2.2	1.92	0.012
O	6	2.81	0.001
Ni	8	3.35	0.018

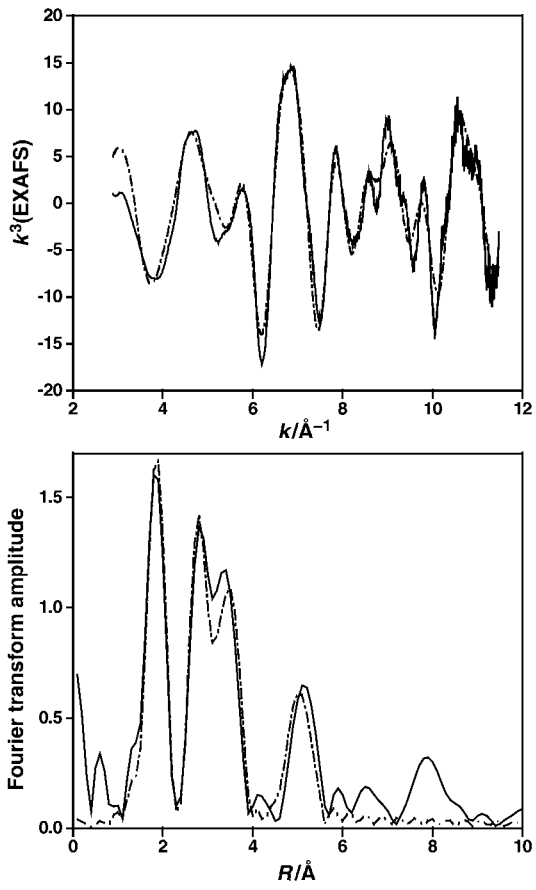

Fig. 8 Co K-edge EXAFS data (top) and corresponding Fourier transform (bottom). The broken line shows the result of the fit.

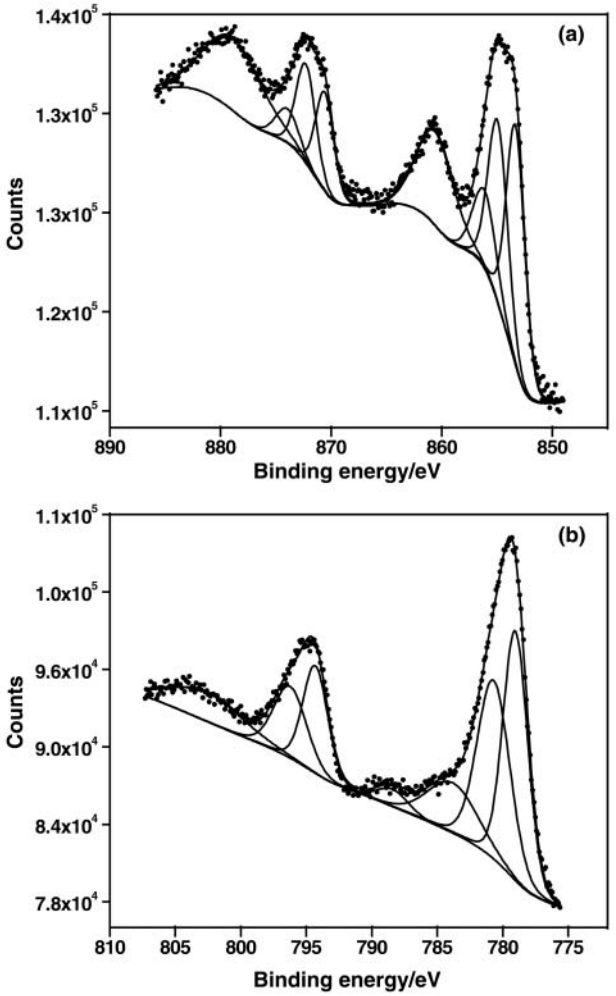

Fig. 9 (a) Ni 2p XPS data, (b) Co 2p XPS data.

1.0 derived from the EXAFS data is also consistent with the neutron diffraction results. Taking into account the difficulties in accurately determining the coordination numbers for EXAFS data the results of the nickel- and cobalt-K edge EXAFS and XANES show good agreement with the neutron diffraction data.

In summary, the neutron diffraction, magnetic, XANES and EXAFS data recorded from $NiCo_2O_4$ prepared by thermal decomposition of metal nitrates suggest a delocalised electron distribution over the cationic Ni octahedral sites originating from the presence of nickel in the unusually high +4 oxidation state and point out a bulk cation distribution of $\{Ni^{3+}{}_{0.1}Co^{2+}{}_{0.9}\}_{tet}[Ni^{3.5+}{}_{0.9}Co^{2.5+}{}_{1.1}]_{oct}O_4$.

(iv) XPS measurements

The Ni 2p spectrum (Fig. 9 (a)) was best fitted considering two spin–orbit doublets characteristic of Ni^{2+} and Ni^{3+} and a third less intense doublet appearing at higher binding energy which, in view of the XANES and EXAFS results, we associate with Ni^{4+} (Table 6). There is a sparsity of XPS data on Ni^{4+}-containing materials. Recently, Xiao and Xu[36] claimed the presence of Ni^{4+} and Ni^{3+} in lithium nickel oxide electrode materials. Although the shape of their Ni XPS spectra resembled the shape of the spectra reported here their quoted binding energies for Ni^{4+} and Ni^{3+} of 854.7 and 852.8 eV, respectively, appear to be extremely low for Ni species in such a high oxidation state.[37–39] Unfortunately, no calibration reference is mentioned and direct comparison is therefore not possible.

The relative areas of Ni^{2+}, Ni^{3+} and Ni^{4+} species are 43, 38.5 and 18.5%, respectively. The intensity of the strong shake-up satellite appearing at higher binding energy than the main $2p_{3/2}$ and $2p_{1/2}$ lines was not taken into account for the calculation of these percentages since it is very difficult to evaluate the exact spectral area transferred from the different Ni contributions. The "average oxidation state" of surface Ni obtained from XPS is *ca.* 2.8 and, as previously found in structurally related materials,[12] is different from that of the bulk. The Co 2p spectrum was fitted in a similar way to that previously used,[12] *i.e.* considering two spin–orbit doublets and three shake-up satellites (Fig. 9(b)). The binding energies obtained from the fit and the assignment of the peaks to different oxidation states of cobalt are shown in Table 7. The results indicated a Co^{3+}/Co^{2+} ratio of 0.76.

We would finally mention that the Co/Ni ratio obtained from the XP spectra is *ca.* 0.9, indicating that the surface of the material shows a clear enrichment in nickel. This has been previously observed in samples of $NiCo_2O_4$ prepared by sol–gel methods[12] and from isopropyl alcohol solutions.[40] The sum of the Co/O and Ni/O atomic ratios was close to 0.75 which is similar to that found previously[12] and which corresponds to the metal/O atomic ratio of the bulk where the stoichiometric Co/Ni ratio is 2.0. As suggested previously,[12] charge balance when $Co/Ni \neq 2.0$ is achieved either by changing the oxidation states of Ni and/or Co surface cations, or by substituting surface O^{2-} by hydroxy groups. It follows from these results that the surface cation distribution is different from that of the bulk.

Table 6 Results of the fit of the Ni 2p X-ray photoelectron spectrum

	Spin–orbit doublet I		Spin–orbit doublet II		Spin–orbit doublet III		Satellite I	Satellite II
	Ni $2p_{3/2}$	Ni $2p_{1/2}$	Ni $2p_{3/2}$	Ni $2p_{1/2}$	Ni $2p_{3/2}$	Ni $2p_{1/2}$		
E_B/eV	853.3	870.6	854.9	872.3	856.1	874.0	860.6	878.9
FWHM/eV	2.0	2.0	2.1	2.1	2.4	2.4	3.9	6.1
I_{rel} (%)	28		25		12		16	19
Assignment	Ni^{2+}		Ni^{3+}		Ni^{4+}			

Table 7 Results of the fit of the Co 2p X-ray photoelectron spectrum

	Spin–orbit doublet I		Spin–orbit doublet II		Satellite I	Satellite II	Satellite III
	Co $2p_{3/2}$	Co $2p_{1/2}$	Co $2p_{3/2}$	Co $2p_{1/2}$			
E_B/eV	779.0	794.3	780.7	796.2	783.8	788.4	802.7
FWHM/eV	2.2	2.2	2.9	2.9	4.5	2.8	6.6
I_{rel} (%)	37		40		11	2	10
Assignment	Co^{3+}		Co^{2+}		Co^{2+}	Co^{3+}	$Co^{2+}+Co^{3+}$

Conclusions

The cation distribution and magnetic structure of $NiCo_2O_4$ prepared by thermal decomposition of metal nitrates has been deduced from magnetic, neutron diffraction, and XANES and EXAFS measurements. The results have shown a delocalised electron distribution on the octahedral sites originating from the presence of nickel in the +4 oxidation state. This unusually high oxidation state of nickel has not been reported before for $NiCo_2O_4$.The examination by XPS of the surface composition has shown that the cation distribution at the surface does not resemble the cation distribution of the bulk. The examination by XPS of the surface composition has shown that the cation distribution at the surface does not resemble the cation distribution of the bulk.

Acknowledgements

The authors acknowledge financial support from the Chilean CONICYT under Projects 7990026 and 1990951 (Cooperación Internacional–Fondecyt), the USACH–CSIC bilateral cooperation programme, the Spanish Dirección General de Enseñanza Superior for the award of travel grants (J. F. M. and M. G.) to Daresbury Laboratory, and the EPSRC for the award of beamtime at Daresbury Laboratory. We also thank EPSRC for additional financial support and the provision of neutron diffraction facilities.

References

1 J. Haenen, W. Visscher and E. Barendrecht, *J. Electroanal. Chem.*, 1986, **208**, 273.
2 B. Marsan, N. Fradette and G. Beaudoin, *J. Electrochem. Soc.*, 1992, **139**, 139.
3 M. R. Gennero de Chialvo and A. C. Chialvo, *Electrochim. Acta*, 1993, **38**, 2247.
4 R. N. Singh, J. F. Koenig, G. Poillerat and P. Chartier, *J. Electroanal. Chem.*, 1991, **314**, 241.
5 N. Heller-Ling, M. Prestat, J. L. Gautier, J. F. Koenig, G. Poillerat and P. Chartier, *Electrochim. Acta*, 1997, **42**, 197.
6 P. Cox and D. Pletcher, *J. Appl. Electrochem.*, 1990, **20**, 549.
7 O. Knop, K. I. G. Reid, Y. Sutarno and Y. Nakamura, *Can. J. Chem.*, 1968, **46**, 3463.
8 M. Lenglet, R. Guillamet, J. Dürr, D. Gryffroy and R. E. Vandenberghe, *Solid State Commun.*, 1990, **74**, 1035.
9 P. D. Battle, A. K. Cheetham and J. B. Goodenough, *Mater. Res. Bull.*, 1979, **14**, 1013.
10 F. K. Lotgering, *Philips Res. Rep.*, 1956, **11**, 337.
11 G. Blasse, *Philips Res. Rep.*, 1963, **18**, 383.
12 J. F. Marco, J. R. Gancedo, M. Gracia, J. L. Gautier, E. Ríos and F. J. Berry, *J. Solid State Chem.*, 2000, **153**, 74.
13 A. C. Larson and R. B. von Dreele, *General Structure Analysis System*, Los Alamos National Laboratory, Los Alamos, NM, 1994.
14 N. Binsted, S. Gurman and J. Campbell, *Laboratory EXCURV90 program*, Daresbury Laboratory, 1990.
15 S. J. Gurman, N. Binsted and I. Ross, *J. Phys. C*, 1984, **17**, 143.
16 J. B. Pendry, *Low Energy Electron Diffraction*, Academic Press, New York, 1974.
17 S. Sasaki, K. Fujino and Y. Takeuchi, *Proc. Jpn. Acad.*, 1979, **55**, 43.
18 X. Liu and C. T. Prewitt, *Phys. Chem. Miner.*, 1990, **17**, 168.
19 R. W. Joyner, K. J. Martin and A. Meehan, *J. Phys. C*, 1987, **20**, 4005.
20 C. D. Wagner, L. E. Davis, M. V. Zeller, J. A. Taylor, R. M. Raymond and L. H. Gale, *Surf. Interf. Anal.*, 1981, **3**, 211.
21 R. E. Watson and A. T. Freeman, *Acta Crystallogr.*, 1961, **14**, 27.
22 W. E. O'Grady, K. I. Pandya, K. E. Swider and D. A. Corrigan, *J. Electrochem. Soc.*, 1996, **143**, 1613.
23 A. N. Mansour and C. A. Melendres, *J. Phys. IV*, 1997, **C2**, 1171.
24 M. Balasubramanian, X. Sun, X. Q. Yang and J. McBreen, *J. Electrochem. Soc.*, 2000, **147**, 2903.
25 A. N. Mansour and C. A. Melendres, *J. Phys. Chem. A*, 1998, **102**, 65.
26 L. R. Furenild, M. W. Renner and E. Fujita, *Physica B*, 1995, **208–209**, 739.
27 M. Crespin, P. Levitz and L. Gatineau, *J. Chem. Soc., Faraday Trans. 2*, 1983, **79**, 1181.
28 J. A. Alonso, M. J. Martínez-Lope and M. A. Hidalgo, *J. Solid State Chem.*, 1995, **116**, 146.
29 J. L. García-Muñoz, M. Suaaidi, M. J. Martínez-Lope and J. A. Alonso, *Phys. Rev. B.*, 1995, **52**, 13563.
30 A. N. Mansour, J. McBreen and C. A. Melendres, *J. Electrochem. Soc.*, 1999, **146**, 2799.
31 A. N. Mansour, X. Q. Yang, X. Sun, J. McBreen, L. Croguennec and C. Delmas, *J.Electrochem. Soc.*, 2000, **147**, 2104.
32 I. Nakai, K. Takahashi, Y. Shiraishi, T. Nakagome, F. Izumi, Y. Ishii, F. Nishikawa and T. Konishi, *J. Power Sources*, 1997, **68**, 536.
33 R. D. Shannon, *Acta Crystallogr. Sect. A*, 1976, **32**, 751.
34 H. Falcón, A. E. Goeta, G. Punte and R. E. Carbonio, *J. Solid State Chem.*, 1997, **133**, 379.
35 A. Rougier, I. Saadonne, P. Gravereau, P. Willmann and C. Delmas, *Solid State Ionics*, 1996, **90**, 83.
36 X. Xiao and Y. Xu, *J. Mater. Sci.*, 1996, **31**, 6449.
37 N. S. McIntyre and M. G. Cook, *Anal. Chem.*, 1975, **47**, 2208.
38 K. S. Kim and N. Winograd, *Surf. Sci.*, 1974, **43**, 625.
39 L. J. Matienzo, L. I. Yin, S. O. Grim and W. E. Schwartz, Jr., *Inorg. Chem.*, 1973, **12**, 2762.
40 L. A. de Faria, M. Prestat, J. F. Koenig, P. Chartier and S. Trasatti, *Electrochim. Acta*, 1998, **44**, 1481.